Studies Concerning the Temporal and Genetic Control of Cell Polarity in *Saccharomyces cerevisiae*

Michael Snyder, Sonja Gehrung, and Barbara D. Page

Department of Biology, Yale University, New Haven, Connecticut 06511

Abstract. The establishment of cell polarity was examined in the budding yeast, *S. cerevisiae*. The distribution of a polarized protein, the SPA2 protein, was followed throughout the yeast cell cycle using synchronized cells and *cdc* mutants. The SPA2 protein localizes to a patch at the presumptive bud site of G1 cells. Later it concentrates at the bud tip in budded cells. At cytokinesis, the SPA2 protein is at the neck between the mother and daughter cells. Analysis of unbudded haploid cells has suggested a series of events that occurs during G1. The SPA2 patch is established very early in G1, while the spindle pole body resides on the distal side of the nucleus. Later, microtubules emanating from the spindle pole body intersect the SPA2 crescent, and the nucleus probably rotates towards the SPA2 patch. By middle G1, most cells contain the SPB on the side of the nucleus proximal to the SPA2 patch, and a long extranuclear microtubule bundle intersects this patch. We suggest that a microtubule capture site exists in the SPA2 staining region that stabilizes the long microtubule bundle; this capture site may be responsible for rotation of the nucleus. Cells containing a polarized distribution of the SPA2 protein also possess a polarized distribution of actin spots in the same region, although the actin staining is much more diffuse. Moreover, *cdc4* mutants, which form multiple buds at the restrictive temperature, exhibit simultaneous staining of the SPA2 protein and actin spots in a subset of the bud tips. *spa2* mutants contain a polarized distribution of actin spots, and *act1-1* and *act1-2* mutants often contain a polarized distribution of the SPA2 protein suggesting that the SPA2 protein is not required for localization of the actin spots and the actin spots are not required for localization of the SPA2 protein. *cdc24* mutants, which fail to form buds at the restrictive temperature, fail to exhibit polarized localization of the SPA2 protein and actin spots, indicating that the CDC24 protein is directly or indirectly responsible for controlling the polarity of these proteins. Based on the cell cycle distribution of the SPA2 protein, a "cytokinesis tag" model is proposed to explain the mechanism of the nonrandom positioning of bud sites in haploid yeast cells.

THE establishment of cell polarity is a fundamental process in eukaryotes. Various eukaryotic cells exhibit polarized cell growth and many cells exhibit polarized divisions, a separate but related process, in which cells undergo division in a specific plane.

Yeast exhibits both polarized cell growth and polarized cell divisions and are useful model organisms for studying these processes. Late in G1 of each cell cycle, a new bud forms at a specific site on the edge of the cell. The bud enlarges throughout the remainder of the cell cycle, and the size of the bud roughly indicates the position of the cell within the cell cycle. Haploid cells and most new **a**/α diploid mother cells preferentially undergo axial budding in which a new bud forms near the old bud site or birth scar (i.e., next to the previous site of cytokinesis) (Freifelder, 1960; Snyder, 1989). Diploid daughter cells exhibit distal budding in which a bud forms on the side of the cell opposite the birth scar. In cells that undergo axial budding a reorientation event occurs during G1. In the beginning of G1, the spindle pole body (SPB)[1] lies distal to the site of cytokinesis. Sometime during G1, it either moves to the opposite side of the nucleus or the entire nucleus rotates so that by the end of G1, the SPB is directly facing the bud, and extranuclear microtubules extend from the SPB into the nascent bud (Byers, 1981). It is not known when during the cell cycle the yeast cell commits to polarized growth, how the cell positions the incipient bud site, or how the SPB/nuclear reorientation occurs.

Several different components have now been identified that accumulate at the incipient bud site. Actin spots concentrate towards one edge of the unbudded cell and within the bud in budded cells (Adams and Pringle, 1984; Drublin, 1990; Kilmartin and Adams, 1984; Novick and Botstein, 1985). The *CDC3*, *CDC10*, and *CDC12* gene products and chitin also accumulate at the presumptive bud site (Kim et al., 1991; Hayashibe and Katohda, 1973); these components remain as a ring surrounding the bud neck and appear to be involved in cytokinesis (Haarer and Pringle, 1987).

The localization of components to the incipient bud site of yeast may be directly or indirectly controlled by several genes that are important for bud formation. Cells with temperature-sensitive mutations in any of three genes, *CDC24*,

1. *Abbreviation used in this paper*: SPB, spindle pole body.

Table I. Strain List

A364A strains (derived from those of Dr. L. Hartwell):	
Y145	*MATa his7 ura1*
Y567	*MATa his7 ura1* *MATα ura3-52 ade2-101 trp1-289 leu2-3,112 can1 sap3 his7*
Y146/Y147	*MATa cdc2-2 his7 ura1* *MATα cdc2-2 his7 hom3 can1 sap3*
Y150/Y151	*MATa cdc5-1 his7 ura1* *MATα cdc5-1 his7 hom3 can1 sap3*
Y561	*MATa cdc13-1 his7 ura1* *MATα cdc13-1 his7 hom3 can1 sap3*
Y562	*MATa cdc14-1 his7 ura1* *MATα cdc14-1 his7 hom3 can1 sap3*
Y563	*MATa cdc15-2 his7 ura1* *MATα cdc15-2 his7 hom3 can1 sap3*
Y564	*MATa cdc16-1 his7 ura1* *MATα cdc16-1 his7 hom3 can1 sap3*
Y565	*MATa cdc17-1 his7 ura1* *MATα cdc17-1 his7 hom3 can1 sap3*
Y566	*MATa cdc28-1 his7 ura1* *MATα cdc28-1 his7 hom3 can1 sap3*
Y585	*MATa cdc4-1 his7 ura1* *MATα cdc4-1 his7 hom3 can1 sap3*
Y588	*MATa cdc24-2 ura1 ade2 ade1 tyr1 gal1 lys2 his7* *MATα cdc24-2 his7 hom3 can1*
Y533	*MATa cdc24-3 ura1 ade2 ade1 tyr1 gal1 lys2 his7*
Y590	*MATa cdc34-1 ura1 ade2 ade1 tyr1 gal1 lys2 his7* *MATα cdc34-1 ura1 lys⁻ ade2 ade1*

(continued)

CDC42, or *CDC43*, fail to form buds at the restrictive temperature but continue to undergo nuclear division (Sloat and Pringle, 1978; Sloat et al., 1981; Adams et al., 1990). Each of these mutants arrests as large round unbudded cells and exhibits a random distribution of chitin and actin. The CDC24 protein is also involved in bud site selection; several temperature sensitive *cdc24* mutants exhibit random budding patterns at the permissive temperature (Sloat et al., 1981). Thus, the CDC24 protein directly or indirectly controls budding in three interrelated ways: the establishment of the incipient bud site, the localization of different components to that site, and the initiation of bud formation.

The SPA2 protein of yeast localizes at the incipient bud site and at sites of cell growth, and it plays a role in budding (Snyder, 1989; Gehrung and Snyder, 1990). In unbudded cells a sharp crescent patch of the SPA2 protein forms at one edge of the cell, and in budded cells the protein localizes to the bud tip. In addition to its polarized localization in vegetatively growing cells, the SPA2 protein exhibits a polarized distribution in yeast cells preparing to mate. When haploid yeast cells are treated with mating pheromone, the cells arrest in late G1 and a projection grows out from one edge of the cells; the SPA2 protein localizes to the tip of the projection. Disruption of the *SPA2* gene results in viable cells that are slightly rounder than wild-type cells. *spa2* mutants exhibit reduced fidelity of axial budding in both haploid cells and diploid cells. They also exhibit defects in pheromone-induced morphogenesis and mating. Thus, the SPA2 protein is important in both polarized growth and polarized cell division.

Since the SPA2 protein is a useful marker for cell polarity, analysis of its distribution throughout the cell cycle can provide clues as to when polarity is first established, and when this polarity is established relative to other cellular events. We also analyzed yeast mutants with lesions in the actin genes or genes involved in budding to determine the role and order of specific gene products in the establishment of cell polarity.

Materials and Methods

Yeast Strains and Media

Yeast strains are listed in Table I. The *cdc* strains are congenic with A364A, the *act1* and *tub2* mutant strains are congenic with S288C, and the *cdc24* strain is congenic with C276. Growth media and standard genetic manipulations are as described (Sherman et al., 1986).

Cell Synchronization

A variety of conditions and strains were tested for synchronization of yeast

Table I. Strain List

C276 congenic strains (from Dr. J. Pringle):	
Y580	*MATa* *MATα*
Y581	*MATa cdc24-4* *MATα cdc24-4*
S288C strains (from Dr. P. Novick, T. Huffaker, this laboratory):	
Y603	*MATα ura3-52 lys2-801 ade2-101 trp1-901 his3-Δ200*
Y559	*MATα act1-2 his4-619*
Y560	*MATα act1-1 his4-619*
Y270	*MATa ura3-52 lys2-801 ade2-101 trp1-901 his3-Δ200* *MATα ura3-52 lys2-801 ade2-101 trp1-901 his3-Δ200*
Y650	*MATa ura3-52 lys2-801 ade2-101 trp1-901 his3-Δ200 spa2-Δ2::TRP1* *MATα ura3-52 lys2-801 ade2-101 trp1-901 his3-Δ200 spa2-Δ3::URA3*
Y630 (TH132)	*MATa ura3-52 lys2-801 ade2-101 his4-539* *MATα ura3-52 LYS2 ADE2 HIS4*
Y631 (TH133)	*MATa tub2-104 ura3-52 ade2-101 his4-539* *MATα tub2-104 ura3-52 ADE2 HIS4*
Y632 (TH134)	*MATa tub2-401 ura3-52 lys2-801 ade2-101 his4-539* *MATα tub2-401 ura3-52 LYS2 ADE2 HIS4*
Y633 (TH135)	*MATa tub2-402 ura3-52 lys2-801 ade2-101 his4-539* *MATα tub2-401 ura3-52 LYS2 ADE2 HIS4*
Y634 (TH136)	*MATa tub2-403 ura3-52 lys2-801 ade2-101 his4-539* *MATα tub2-403 ura3-52 LYS2 ADE2 HIS4*
Y635 (TH137)	*MATa tub2-404 ura3-52 lys2-801 ade2-101 his4-539* *MATα tub2-404 ura3-52 LYS2 ADE2 HIS4*
Y636 (TH138)	*MATa tub2-405 ura3-52 lys2-801 ade2-101 his4-539* *MATα tub2-404 ura3-52 LYS2 ADE2 HIS4*

cells using α-factor. Optimal conditions were found using haploid strain Y145 (A364A background), and the following treatment. 25 ml of yeast cells were grown at 30°C in YPD media to OD (600) = 0.3. α-Factor (Sigma Chemical Co., St. Louis, MO) was added to 3 μg/ml (75 μg total), and after incubation for 45 min at 30°C another 75-μg aliquot of α-factor was added. After incubation for an additional 45 min, the cells were harvested by centrifugation in a JA20 rotor (Beckman Instruments Co., Fullerton, CA) at 7,000 rpm (5,900 *g*) for 2 min at room temperature. The cells were washed three times in 25 ml YPD media that was prewarmed at 30°C, resuspended in warm 25 ml YPD media, and incubated with shaking at 30°C. 3-ml aliquots were removed at the following times: 0, 30, 45, 55, 65, 75, 85, 95, 105, 115, 125, 135, and 145 min. Cells were fixed by the addition of formaldehyde to 3.7% (vol/vol) final concentration and incubated with shaking for 1 h and 10 min at room temperature. After fixation, cells were washed and processed for indirect immunofluorescence as described previously (Gehrung and Snyder, 1990). Significantly poorer cell synchrony was observed if cells were incubated with α-factor for longer periods of time. The experiment with the best cell synchrony is shown in Figs. 2–4. Qualitatively similar results were found for three other experiments.

Cell Cycle Arrest

Yeast cells were grown at the permissive temperature, 24°C for the *cdc* mutants and 20–22°C for *act1* mutants, until OD (600) ~0.3. A 5-ml culture was shifted to the restrictive temperature at 37°C; *cdc* mutants were incubated for 2–2.5 h at this temperature and *act1* mutants were incubated for 1 h. Parallel cultures of each mutant strain were incubated at the permissive temperature to serve as a control. Congenic wild-type strains were subjected to the temperature shift to provide additional controls (see strain list). At the end of the incubation period, cells were fixed by adding formaldehyde to 3.7% (vol/vol) final concentration, and the culture was incubated for 1 h with shaking at room temperature. The cells were then washed and processed for indirect immunofluorescence.

To prepare stationary phase cells, an exponentially growing culture of yeast cells at OD (600) = 0.2 was divided into three 5-ml aliquots and incubated at 30°C. One culture was harvested by centrifugation after 24 h, another after 48 h, and the third after 72 h.

Immunofluorescence

Immunofluorescence was performed as described previously (Gehrung and Snyder, 1990) using anti-SPA2 antibodies and anti-tubulin antibodies. The preparation of spheroplasts involved incubation at 37°C for 45 min to 1 h with 5 μg/ml Zymolase 0.02% glusulase (Dupont Co., Wilmington, DE) as described. However, in the experiment using stationary phase cells the amount of zymolyase and glusulase was doubled for cells prepared from the 24-h culture (final concentrations: 10 μg/ml Zymolase 0.04% glusulase) and increased 3.5-fold for cells from the 48- and 72-h cultures (final concentrations: 17.5 μg/ml Zymolase 0.07% glusulase). For *cdc* and stationary phase cells, affinity-purified rabbit anti-SPA2 antibodies (Snyder, 1989) were detected with rhodamine or Texas Red-conjugated secondary antibodies (Cappel Laboratories, Malvern, PA and Amersham Chemical Co., Arlington Heights, IL, respectively); tubulin was identified with a rat mAb YOL1/34 (Kilmartin et al., 1982) and fluorescein-conjugated goat anti-rat antibodies (Cappel Laboratories).

For the synchronized cell experiments, two types of tubulin antibodies were used. YOL1/34 was used to stain one aliquot of fixed cells. The SPA2 and tubulin staining regions were distinguished by a Texas Red-conjugated donkey anti-rabbit antibody to detect the SPA2 staining region and fluorescein-conjugated goat anti-rat antibodies to detect the anti-tubulin antibodies. A separate aliquot of fixed cells was stained with a rabbit anti-tubulin antibody (Bond et al., 1986). This antibody is very high titer and allows

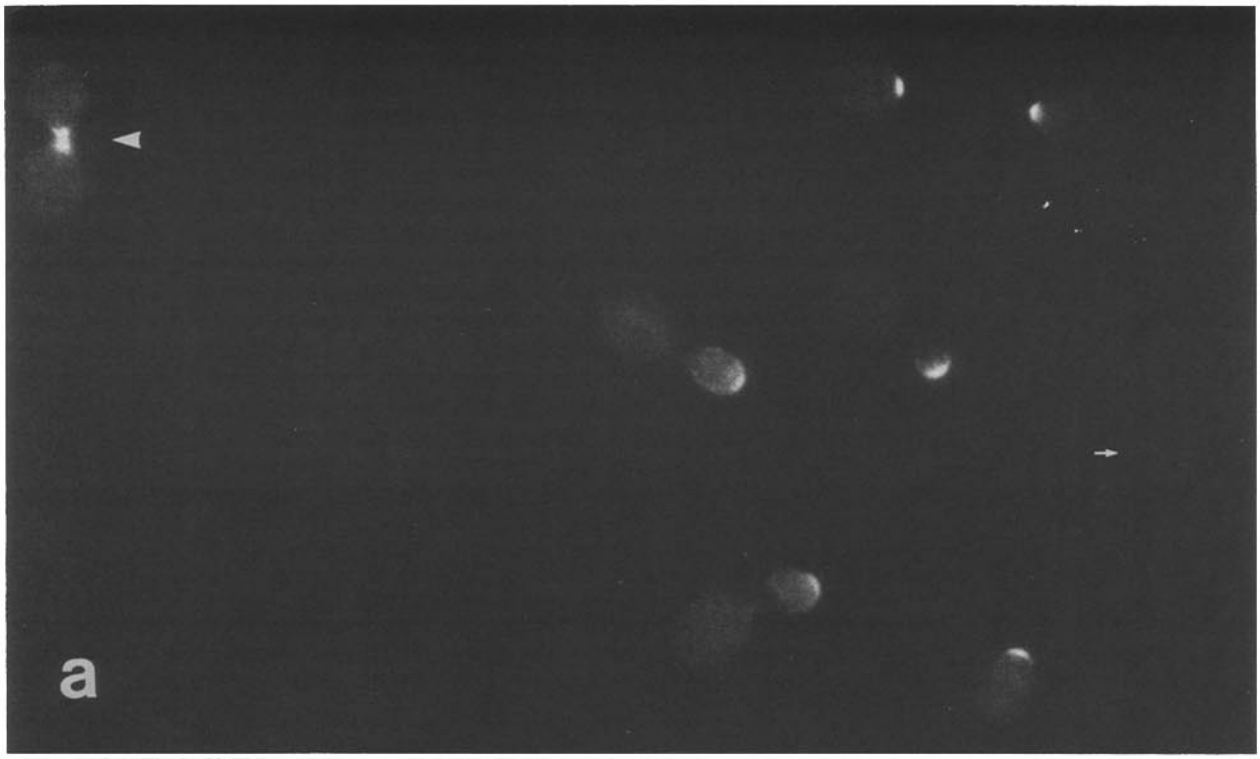
a

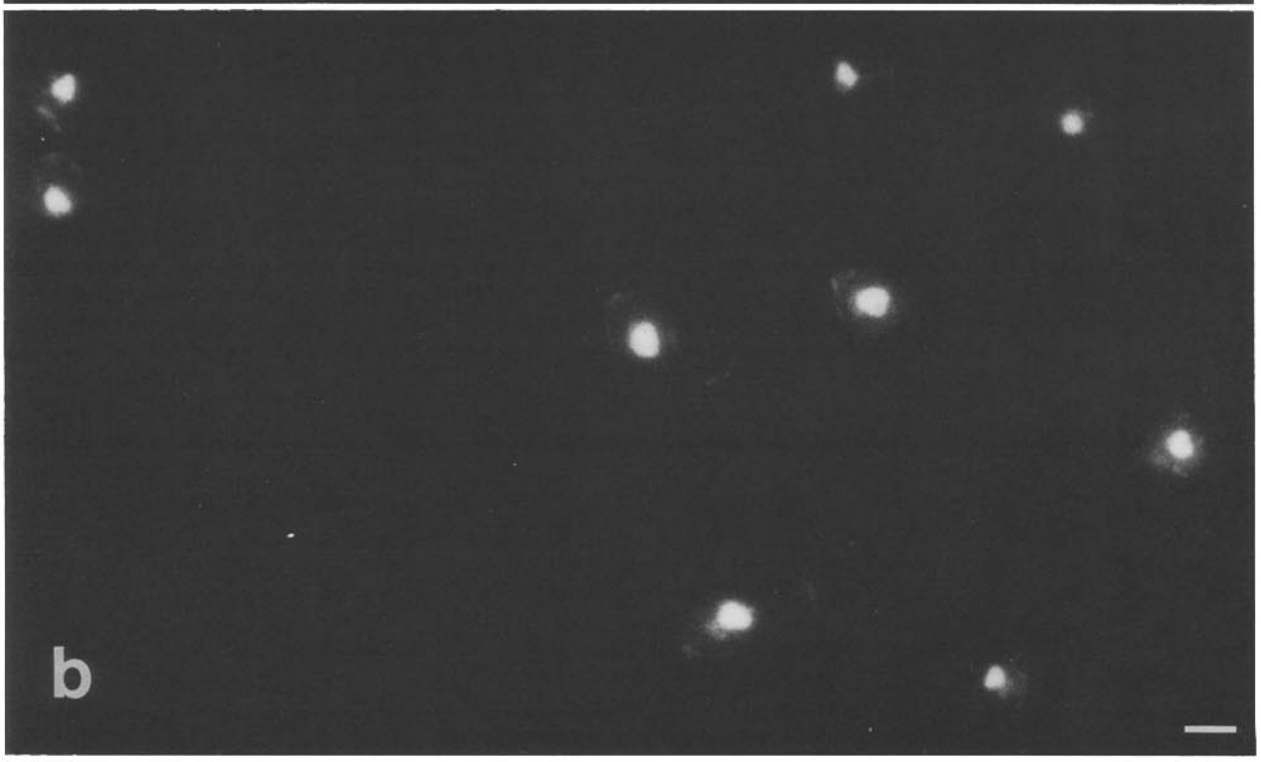
b

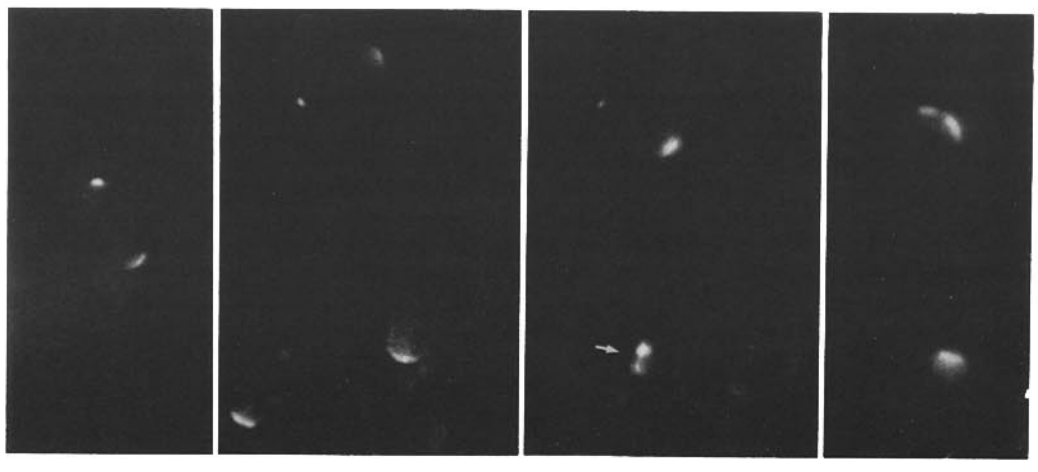
c

easy visualization of microtubules in yeast. Both SPA2 and tubulin were detected with Texas Red–conjugated donkey anti-rabbit antibodies. The SPA2 and tubulin regions are readily distinguished by their different localization patterns.

Double-labeling experiments with anti-SPA2 antibodies and rhodamine-conjugated phalloidin, which binds F-actin were performed as described previously (Gehrung and Snyder, 1990). Detection of the bound anti-SPA2 antibodies was with fluorescein-conjugated goat anti-rabbit antibodies. Optimal double-labeling experiments with both anti-SPA2 antibodies and rhodamine-conjugated phalloidin was achieved by reducing the zymolyase/glusulase-treatment step to 30 min instead of 1 h. This resulted in a reduced SPA2 staining signal, perhaps due to impaired permeability to the antibodies, but significantly improved the phalloidin staining.

Quantitation of Synchronized Cells

Cells from various timepoints after synchronization with α factor were scored as described in the text and Figs. 3 and 4 with the following comments: (*a*) For determining the frequency of budded cells and spindles, between 100–302 cells were counted for each timepoint (mean 197). For determining the different types of unbudded cells, additional unbudded cells were scored for most of the timepoints. 95–164 unbudded cells were scored for each timepoint (mean 147). (*b*) Because the same secondary antibody was used for the quantitation in Fig. 3, it is possible that many of the unbudded cells had a small SPA2 patch, but were oriented in such a way that the SPA2 patch overlaps with an intense microtubule staining, for example the SPB region. These cells would be scored as lacking a SPA2 patch. This situation either does not occur or is very rare because we also quantitated the frequency of cells in the different categories shown in Fig. 4 using cells that were stained with SPA2 antibodies and YOL1/34 and two different secondary antibodies. The results were in close agreement with those shown in Fig. 3 *C*. Much greater preference was given to the results obtained with the rabbit tubulin antibody, because its high titer allowed easy detection of microtubule bundles and therefore reliable determination as to whether the bundles intersected the SPA2 staining region. We also note that since we do not know the limit of detection of the antibodies used, it is possible that single or low numbers of microtubules will not be detected in these experiments.

(*c*) The SPB was scored as residing either on the side of the nucleus proximal to the SPA2 patch or on the distal side. In <15% of the cells, the SPB lay approximately in the center: 50% of these cells were counted as proximal and 50% were scored as distal.

(*d*) As described in the text, a major concern was the separation of buds from the mother cells which would result in scoring mother cells as unbudded cells lacking a SPA2 staining region. Therefore, cells were manipulated as carefully as possible to avoid the separation. Bud heads are generally easy to recognize because of the broad SPA2 staining at the tip, and are therefore easy to quantitate within the sample. Based on the frequency of detached buds that were observed, mother cells that had lost buds were estimated to comprise 32, 16, and 33% of the cells which did not stain with SPA2 at the 65-, 75-, and 125-min timepoints (where the number of unbudded cells is very low); this value is estimated to be <0.8% of the total unbudded cells at the other timepoints. These values were subtracted from the unbudded cells without a SPA2 stain (Fig. 3 *C*). These corrections do not alter the overall trends noted in the figure. (Note: a small fraction of large-budded cells lack SPA2 staining at the tip; the detached buds of these cells would be difficult to score in our analysis. However, since cells lacking SPA2 staining at the bud tip comprise a small fraction of the total population [<5%] at any given time point we estimate their contribution to be very minor. Moreover, large budded cells lacking SPA2 staining at the bud tip are usually at cytokinesis and contain staining at the neck. Such cells would usually be scored as SPB distal, MT → SPA2 in Fig. 3 *C*.)

(*e*) Cells with very short spindles (see legend to Fig. 3) may be slightly underrepresented because an unfavorable orientation of the cells may not reveal closely spaced SPBs. Nevertheless, scoring these cells still aids in the assessment and analysis of the cell synchrony. (*f*) One method to crudely estimate the length of time it takes for cells to form a SPA2 patch is to first determine the mean time for cells to reach cytokinesis as judged by staining at the neck with anti-SPA2 antibodies. This value (84.0 min) is then compared to that of the mean time of the accumulation of cells that lack a SPA2 patch (86.5 min). (These values were determined using data from the 55-115-min timepoints). The 2.5-min difference approximates about one half the average length of time a cell uses to form a patch after cytokinesis. We note that this figure applies to cells that initially do not have a SPA2 patch and then form one; a different value may exist for cells that do not lose their patch before forming a second one. We have also quantitated the rate with which unbudded cells containing a SPA2 patch appeared in the population relative to the total number of unbudded cells. This value also suggests that a new patch forms within 5 min after cytokinesis.

Immunoblot Analysis

Protein extracts were prepared in an identical fashion to that described previously (Snyder, 1989). Briefly, 5-ml cultures of cells were harvested, washed, and resuspended in 125 μl of lysis buffer containing SDS and protease inhibitors. An equal volume of glass beads was added, and cells were vortexed vigorously for 3 min. The samples were heated to 70°C for 2 min and ~5 μg of protein was loaded onto a 7.0% acrylamide gel containing SDS (Laemmli, 1970). Equal amounts of protein were loaded as judged by analysis of a Coomassie blue stained gel. (Note that although the *cdc* mutants arrest at different positions in the cell cycle, most of the protein bands appear very similar allowing an easy comparison of the different gel samples.) After electrophoresis, proteins were blotted onto nitrocellulose filters (Burnette, 1981), and gel blots were probed with affinity-purified anti-SPA2 antibodies (Snyder, 1989). Bound antibodies were detected with ^{125}I-labeled protein A (>30 mCi/mg; Amersham Chemical Co.).

Results

Distribution of the SPA2 Protein in an Asynchronously Growing Population of Yeast Cells

The initial goal of these studies was to determine the cell cycle distribution of the SPA2 protein using synchronized cells and cdc mutants. To carry out these experiments, we used a different yeast strain, A364A, than the S288C strains of previous studies, primarily for two reasons; significantly greater cell synchronization was achieved using the A364A background and many of the *cdc* mutants are in this strain background (Hartwell, 1974).

When an asynchronous population of either haploid or diploid A364A yeast cells is stained with affinity-purified anti-SPA2 antibodies, results similar, but not identical, to those previously described are observed. In 95–97% of unbudded cells the SPA2 protein localizes to a sharp crescent-shaped patch on the edge of the cell. In budded cells, the SPA2 protein is at the tip of the bud; some cells with a very large bud exhibit more diffuse staining throughout the entire bud (these represent <1% of total budded cells). Many large budded cells that contain completely separated nuclei and are presumably at cytokinesis, stain at the neck between the

Figure 1. Staining of wild-type A364A cells with anti-SPA2 antibodies. A culture of asynchronous diploid Y567 cells were harvested and stained with affinity-purified anti-SPA2 antibodies and detected with fluorescein-conjugated secondary antibodies. (*a*) Anti-SPA2 antibody stain (*Fluorescein*); (*b*) Hoechst 33258 DNA stain of the same cells. The arrowhead indicates a cell at cytokinesis; note the nuclei have completely separated to opposite ends of the cell. In total >200 cells with this morphology and staining pattern have been observed. The small arrow indicates an unbudded cell lacking SPA2 staining. (*c*) Cells containing double SPA2 patches. The leftmost three panels are diploid Y567 cells. The small arrow indicates a cell with side-by-side patches. The rightmost panel contains haploid cells (Y145); the top cell contains a double patch. These haploid cells were from the 75-min timepoint (see next figure) and were stained with Texas Red–conjugated secondary antibodies. (Note in the top cells a microtubule bundle intersects the brightest of the two patches: data not shown). Bar, ~3 μm except rightmost panel of *C*, ~2 μm.

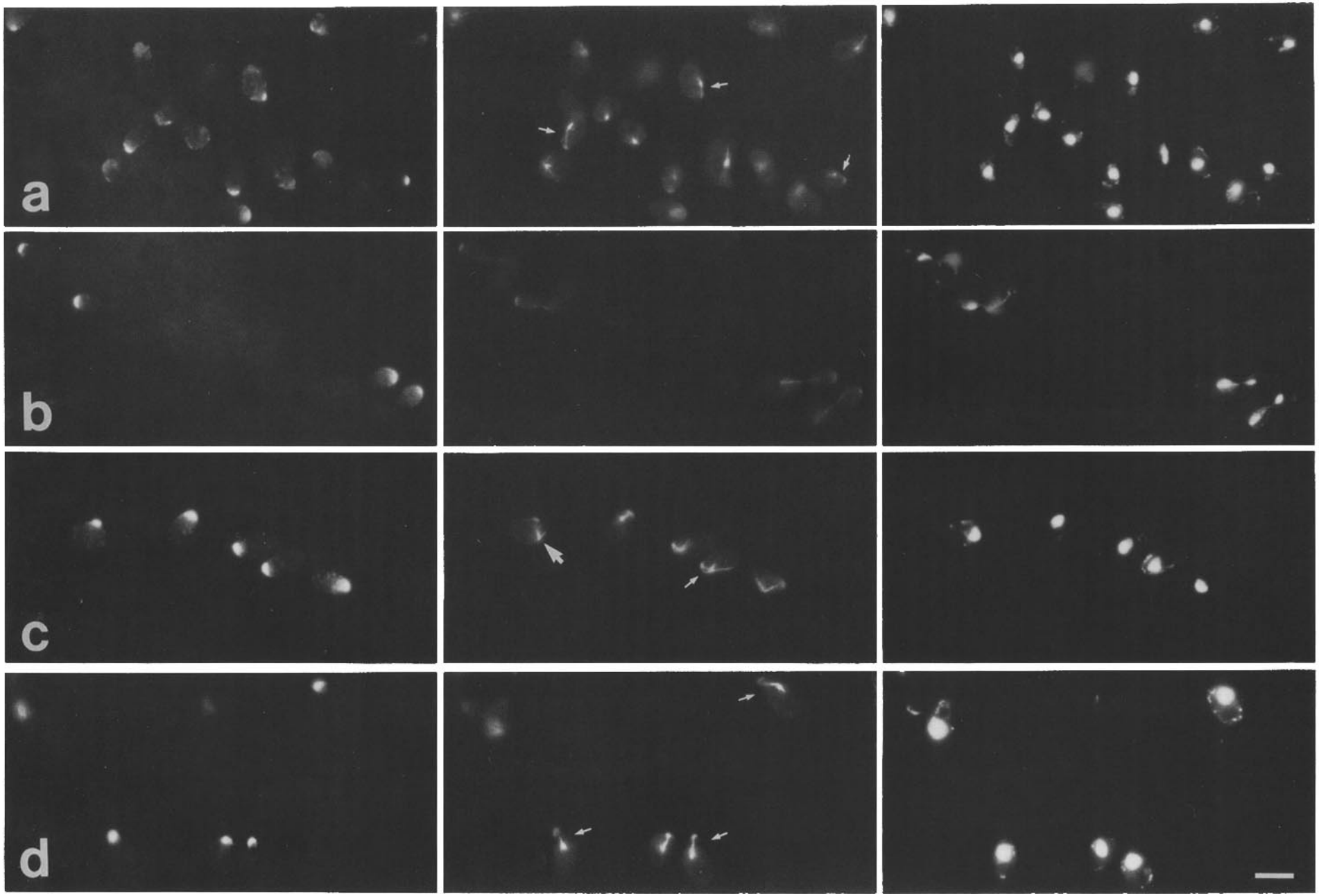
a
b
c
d

mother and daughter cells; this staining is usually weaker than the SPA2 patch in cells at other stages of the cell cycle. A small fraction of the unbudded cells contain more than one SPA2 crescent (this value is <2% of unbudded haploid cells and 5–10% for unbudded diploids). In haploid cells and some diploid cells the two crescents lie adjacent to one another; the majority (~70%) of diploid cells with two SPA2 crescents contain these crescents at opposite ends of the oval (Fig. 1 *C*). No staining is observed at any of the different cellular locations in *spa2-2* and *spa2-3* cells (data not shown). The *spa2-2* and *spa2-3* mutant cells each contain a large substitution of the *SPA2* gene with a selectable marker, leaving only 39 codons of SPA2 coding sequence upstream of the substituted gene (Gehrung and Snyder, 1990).

The simplest explanation for these results is that the SPA2 patch localizes to the incipient bud site in unbudded cells and to the bud tip in budded cells (Snyder, 1989). In addition, the SPA2 protein localizes to the site of cytokinesis. In G1 the cytokinesis site probably does not always completely disappear before the development of a new patch, resulting in unbudded cells with double patches. This hypothesis is consistent with the cell cycle studies described below.

Distribution of the SPA2 Protein in Synchronized Cells

To learn more about when polarity of the SPA2 protein is established in the cell cycle, synchronized yeast cells were prepared and analyzed. *MATa* cells were arrested in G1 with α-factor, washed to remove the pheromone, and then resuspended in fresh media. Aliquots of synchronized cells were harvested at various time intervals and prepared for indirect immunofluorescence. The distribution of the SPA2 protein was examined from cells grown over a period of one and one-half cell divisions (145 min) including one entire G1 period. Cells were simultaneously stained with anti-tubulin antibodies, which allowed further assessment of the cell synchronization and which also served as a positive control for the antibody staining (see Materials and Methods and legends to Figs. 2 and 3). Examples of synchronized cells from several of the timepoints are shown in Fig. 2.

For each timepoint, the percentage of unbudded, small budded and large budded cells was determined (Fig. 3 *A*). Small budded cells are scored as those cells in which the bud is less than one-half the size of the mother cell; large budded cells are those cells in which the bud is more than or equal to one-half the size of the mother cell. We also quantitated the number of cells that contained short spindles and long spindles (Fig. 3 *B*; see legend). The maximum number of budded cells was found at 65 min, the number of unbudded cells continued to rise until a maximum at 105 min and decreased to a minimum at 135 min. Thus, the 65–135-min interval encompasses an entire G1 period for most of the population.

As shown in Figs. 2 and 3, cells treated with α-factor arrest as unbudded cells with a projection. The SPA2 protein localizes to the tip of the projection in >95% of the cells as described previously (Snyder, 1989; Gehrung and Snyder, 1990). However, only in ~40% of the cells is the SPA2 protein sharply localized to the tip; in the remainder of the cells the SPA2 staining is more diffuse in the tip region. This diffuse staining is quite reproducible and is rarely observed in the S288C strains; it is reminiscent of the FUS1::β-galactosidase staining pattern (Trueheart et al., 1987). After cells are released from the α-factor block the SPA2 protein sharply localizes to the tip in a pattern similar to that seen in Fig. 2 *C* (30 and 45 min, not shown). Intense staining is observed at the bud tip of the small budded cells (45 and 55 min in cell cycle 1; and 135 min in cell cycle 2; shown for the 135-min time point). In the large budded cells staining also appears at the tip (65, 75 and 145 min; shown for 65 min) and in many cells undergoing cytokinesis staining is observed at the neck (75 and 85 min; not shown). These results are consistent with observations of asynchronous cultures.

Most unbudded cells contain a SPA2 patch. However, during a short interval at the beginning of G1 a significant fraction of unbudded cells do not stain with anti-SPA2 antibodies. This occurs when the first unbudded cells are beginning to form after cytokinesis (Fig. 3 *C*), and corresponds to <3.5% of the total cells in the population (see Discussion). As new unbudded cells begin to form (65 min, and particularly 75 and 85 min) a small number of cells with two SPA2 crescents are observed (Fig. 1 *C*). This fraction, which constitutes <5% of the unbudded cells at these times, is difficult to quantitate precisely because of ambiguities in distinguishing single and double patches in many cases. These results indicate that a new SPA2 patch forms very early in the cell cycle, probably within 5 minutes after cytokinesis (see Materials and Methods), and in many cases forms before disappearance of the old patch.

Formation of the SPA2 Patch Relative to Spindle Pole Body/Nuclear Reorientation and Extranuclear Microtubule Bundles

After cytokinesis in haploid cells, the spindle pole body is on the side of the nucleus distal to the site where the next bud will form (see Byers, 1981; Freifelder, 1960). At the G1/S boundary, it is oriented towards the nascent bud and extranuclear microtubules emanating from the SPB will extend towards the bud tip (Byers, 1981). To determine the temporal order of events: (*a*) SPB/nuclear reorientation, (*b*) microtubule extension toward the nascent (or incipient) bud site, and (*c*) appearance of the SPA2 patch (as a marker for the incipient bud site), we carefully analyzed the unbudded cells in the synchronized population. Particular attention was paid

Figure 2. Examples of synchronized cells at the various timepoints. *MATa* yeast cells (Y145) were synchronized with α-factor. Examples of cells at four different time points are shown. (*Left*). Anti-SPA2 stain (detected with Texas Red). (*Middle*) Tubulin stain (detected with fluorescein). (*Right*) DNA stain (Hoechst 33258). The SPA2 staining is very intense as compared with the tubulin staining; some crossover of SPA2 signal (which is still red) is consequently observed using the fluorescein filters. (*a*) 0 min after release from α-factor (cells with projections). Cells with arrows have sharp staining at the projection tip; most of the other cells exhibit more diffuse staining in this region. (*b*) 75 min. (*c*) 105 min. Large arrow: a cell with no microtubule bundle intersecting the SPA2 staining region. The other cells all contain intersecting microtubules and have their spindle poles proximal to the SPA2 staining region (microtubules in the rightmost cell are slightly out of the plane of focus). The small arrow indicates a cell with two microtubule bundles intersecting the SPA2 staining region). (*d*) 115 min. Arrows indicate cells with small buds. All contain microtubules intersecting the SPA2 staining region although the plane of focus is not favorable for the leftmost cell. Bar, ~3.8 μm.

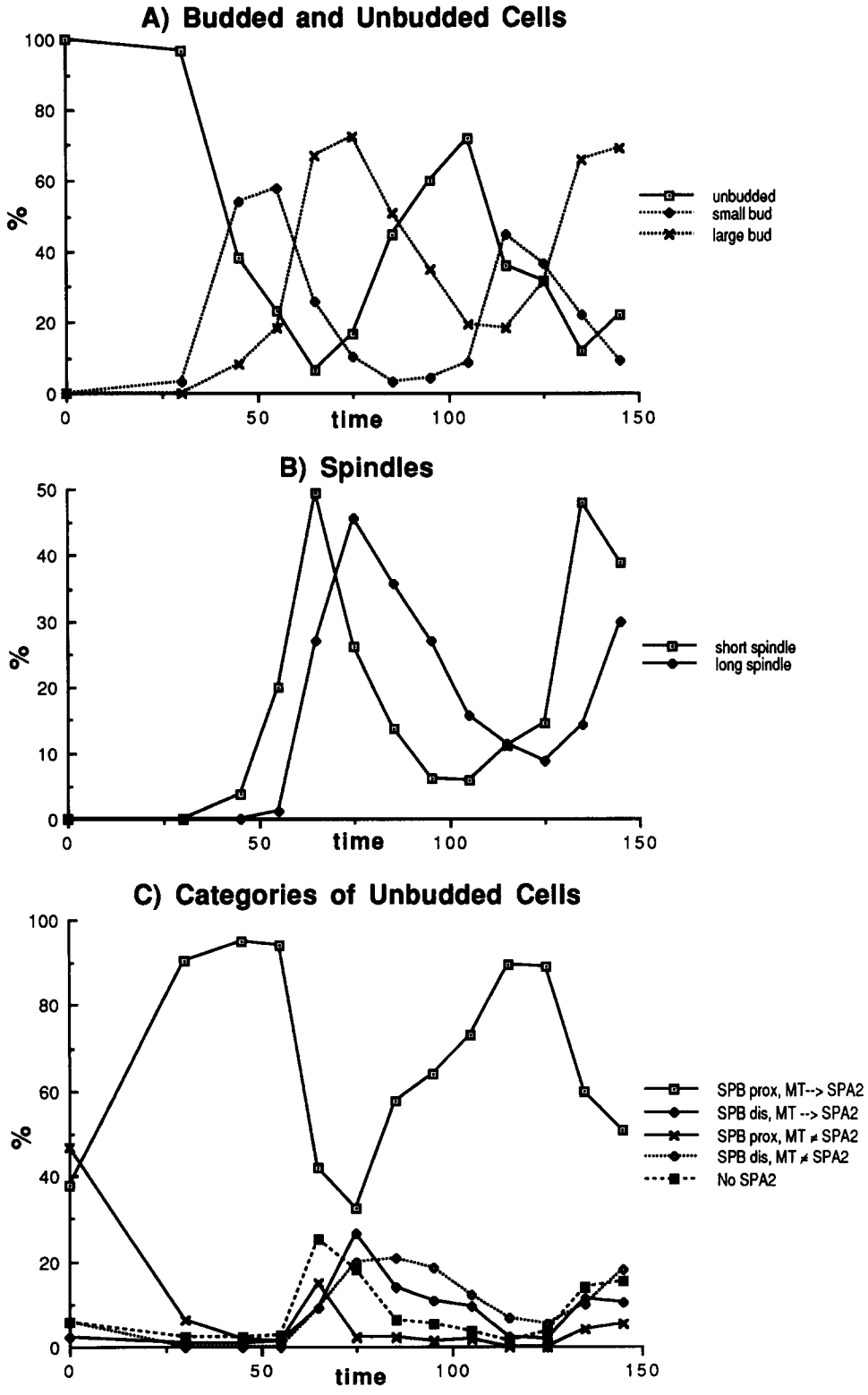

Figure 3. Quantitation of the cell synchronization experiment. (*a*) Percent unbudded, small budded, large budded, and total budded were determined as a function of time after release from α-factor arrest as described in the text and Materials and Methods. (*b*) Percent of short and long spindles. (*Short spindles*) Configurations such as side-by-side spindle poles up to those where the spindle spans the entire nucleus, but the nucleus has not begun elongation. (*Long spindles*) Configurations in which the nucleus has begun elongation up until cytokinesis when the spindle begins dissolving. (*c*) Percentage of unbudded cells containing various configurations of SPA2 staining, SPB orientation, and microtubules intersecting the SPA2 staining region. See Fig. 4 for examples of the different classes. ■, no SPA2 stain, ◇, SPB distal to SPA2; microtubules do not intersect SPA2 staining region (MT≠SPA2), ◆, SPB distal to SPA2, microtubules intersect SPA2 staining region (MT→SPA2); ×, SPB proximal to SPA2, microtubules do not intersect SPA2 staining region; ⊡, SPB proximal to SPA2, microtubules intersect SPA2 staining region.

to the 65–135-min interval which encompasses the entire G1 period of most of the population. Examples of the various types of unbudded cells are shown in Fig. 4, and the frequency with which they occur in the unbudded population is quantitated in Fig. 3 *C*.

As stated above, cells that do not stain with anti-SPA2 antibodies (Fig. 4 *A*) are prevalent in the unbudded population only very early in G1 (65 and 75 min). Cells that stain with SPA2 (Fig. 4, *B–J*) are abundant throughout most of G1 (particularly 85 through 125 min). Of the SPA2 staining cells,

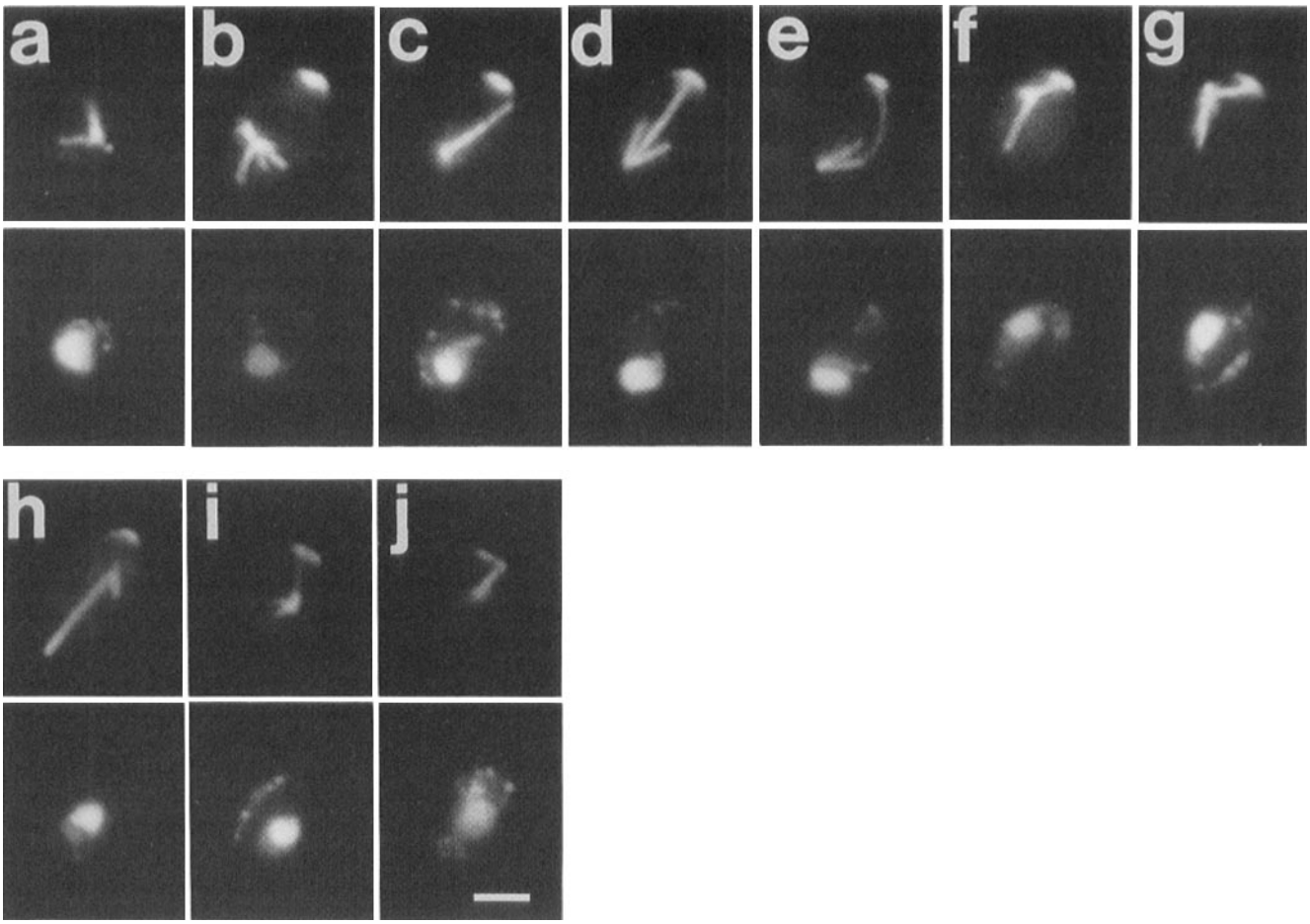

Figure 4. Examples of the different classes of unbudded cells. (*a*) No SPA2 stain, (*b* and *c*) SPB distal to SPA2, microtubules do not intersect SPA2 staining region (note cells like those shown in *c* are very rare; microtubules this long usually intersect the SPA2 staining region). (*d* and *e*) SPB distal to SPA2, microtubules intersect SPA2 staining region. (*f* and *g*) SPB proximal to SPA2, microtubules intersect SPA2 staining region. (*h*) SPB proximal to SPA2, microtubules do not intersect SPA2 staining region. (*i* and *j*) Cells with double SPA2 patches, the microtubule bundles intersect the SPA2 staining region. These cells are treated with anti-SPA2 antibodies and high titer anti-tubulin antibodies; both antibodies are detected with Texas red-conjugated secondary antibodies. In general, cells with long extranuclear bundles that do not intersect the SPA2 staining region (*c* and *h*) are very rare. The Hoechst 33258 stain of the same cell is shown beneath each top panel. Bar, ~1.7 μm.

those that contain the spindle pole on the side of the nucleus distal to the SPA2 patch (Figs. 4, *B–E*) are most prevalent in populations with cells in the earlier portions of G1 (75, 85, and 95 min) and are rare by late G1 (105, 115, and 125 min). These cells usually have a weak Hoechst staining region of the nucleus, presumably the nucleolus, distal to the SPB (difficult to see in the figure). Many of these cells do not contain a long extranuclear microtubule bundle that intersects the SPA2 staining region (Figs. 4, *B* and *C*), whereas others do have a SPA2-intersecting bundle (Fig. 4, *D* and *E*). Cells that contain the spindle pole on the SPA2-proximal side of the nucleus and have an extranuclear microtubule bundle intersecting the SPA2 patch begin accumulating very early in G1 and comprise >60% of the unbudded population by the 85-min timepoint. By late G1 they comprise 90% of this population. Occasionally, cells with two microtubule bundles that intersect the SPA2 staining region are observed (Fig. 2 *C*). Cells that contain the spindle pole body on the side of the nucleus proximal to the SPA2 patch, but do not contain an extranuclear bundle that intersects the patch are extremely rare; in fact, they are only prevalent in cells arrested with α-factor and, to some extent, in cells at the 65-min timepoint.

One simple model that incorporates many of these results is that (*a*) the SPA2 patch forms very early in G1 while the SPB is still on the side of the nucleus distal to the SPA2 patch. (*b*) A long extranuclear microtubule bundle emanates from the SPB and intersects the SPA2 staining region. (*c*) The nucleus rotates such that the SPB is oriented towards the SPA2 staining region. Alternative pathways probably also exist and are described in detail in the discussion.

Relative Localization of the SPA2 Protein and Actin throughout the Yeast Cell Cycle

Both actin spots and the SPA2 protein concentrate in the region of the incipient bud site (Drubin, 1990; Gehrung and Snyder, 1990; Novick and Botstein, 1985) (see below). To

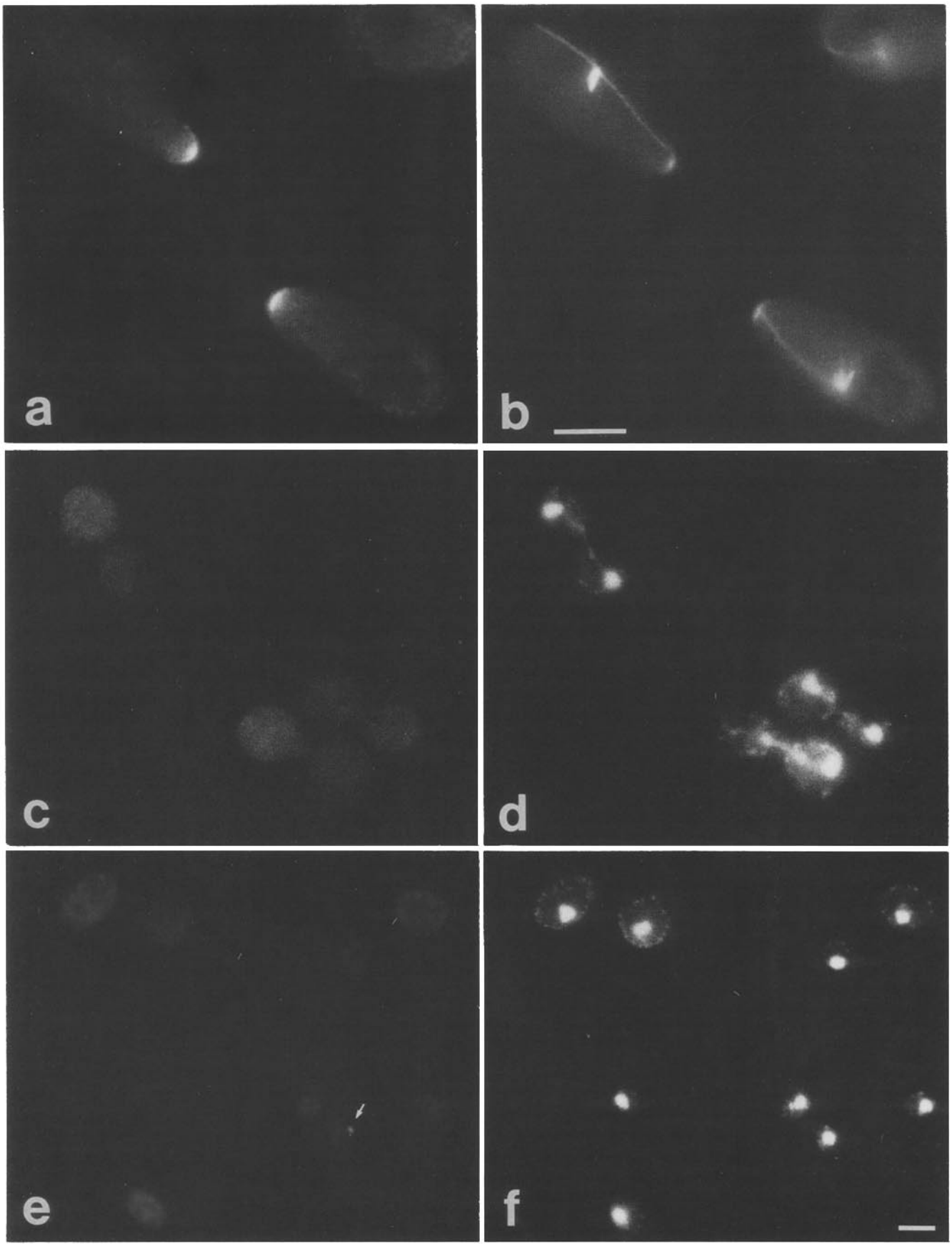

Figure 5. *cdc*-arrested cells and stationary phase cells stained with anti-SPA2 antibodies. Cells were arrested as described in Materials and Methods and stained by indirect immunofluorescence with anti-SPA2 antibodies (*left*, *a*, *c*, and *e*), anti-tubulin antibodies (*b*) and Hoechst (*d* and *f*). Top: (*a* and *b*) *cdc28* arrested cells (*Y566*). (*Middle*) (*c* and *d*) *cdc14*-arrested cells (*Y562*). (*Bottom*) (*e* and *f*) stationary phase cells (*Y567*) incubated for 48 h. One cell in the field contains a faint SPA2 patch (*arrow*). All cells stain with anti-tubulin antibodies (not shown for *cdc14*-arrested or stationary phase cells) and with Hoechst 33258 (not shown for *cdc28*-arrested cells which contain a single nucleus). Approximately 95% of the *cdc14*-arrested cells contain nuclei completely extended between mother and daughter cells although in the bottom cell of the panel the nucleus has not completely extended. Bars, (*a* and *b*) ~4 μm; (*c–f*) ~3.5 μm.

determine the temporal order in which these proteins accumulate at this site, yeast cells were synchronized with α-factor as above and stained with both anti-SPA2 antibodies and rhodamine-conjugated phalloidin, which binds F-actin. Budded cells accumulate actin spots in the bud. All unbudded cells that contain a SPA2 patch also contain a polarized distribution of actin spots at the same end of the cell, and cells with a polarized distribution of actin spots contain a SPA2 patch. (More than 100 unbudded cells were examined at each G1 time point; data not shown; see below for actin staining patterns.) Thus, at this temporal resolution we cannot distinguish a population of cells that contains a polarized localization of only one protein and not the other, suggesting a simultaneous or near simultaneous arrival of both actin and the SPA2 protein at the incipient bud site.

Distribution of the SPA2 Protein in cdc-Arrested Cells and Stationary-Phase Cells

To further analyze the distribution of the SPA2 protein throughout the yeast cell cycle, we examined the localization of the SPA2 protein in various *cdc* mutants that arrest at specific points in the cell cycle (Hartwell, 1974; Pringle and Hartwell, 1981). Diploid *cdc* mutants that arrest as unbudded cells at late G1 (*cdc28-1*), and those that arrest as large budded cells blocked at various times during nuclear division (*cdc2-1*, *cdc5-1*, *cdc13-1*, *cdc14-1*, *cdc15-2*, *cdc16-1*, *cdc17-1*) were grown at the permissive temperature, shifted to the restrictive temperature (37°C) for 2.5 h, fixed, and stained with anti-SPA2 antibodies and with YOL1/34, an anti-tubulin antibody. In one set of control experiments, wild-type diploid cells were treated in an identical fashion. In another set of control experiments, *cdc* cells were incubated at the permissive temperature.

The staining pattern for wild-type cells or for *cdc* cells incubated at the permissive temperature is similar to that of Fig. 1, although in general the signal is slightly diminished for cells grown at 37°C. (The signal is estimated to be two to threefold less, based crudely on film exposure times, and may be either the result of increased fixation when cells are initially at the higher temperature or that there is less SPA2 protein in cells grown at 37°C.) *cdc28-1* mutants, which block in late G1, arrest at the restrictive temperature with one end of the cell elongated; SPA2 staining is at the elongated tip in every cell (Fig. 5) (>200 cells examined). Each of these cells have the SPB on the side of the nucleus proximal to the SPA2 patch and contain one or more long extranuclear microtubule bundles. At least one of these bundles intersects the SPA2 staining region in every cell, and sometimes two microtubule bundles intersect this region. *cdc2*, *cdc5*, *cdc13*, *cdc14*, *cdc15*, *cdc16*, and *cdc17* mutants which are blocked at various points during nuclear division, all arrest as large budded cells (*cdc14* cells shown in Fig. 5). No localized SPA2 staining is detected in any of these mutants, although a low level of enhanced staining is often observed throughout the bud (>150 cells observed for each mutant strain). Microtubules were readily detected with anti-tubulin antibodies, indicating that antibodies were still able to penetrate these cells.

To test whether cells in G_0 contain a SPA2 patch, stationary phase cells were analyzed. Identical yeast cultures were incubated for 24, 48, or 72 h, fixed, and stained by indirect immunofluorescence with anti-SPA2 antibodies. As shown in Fig. 5 and Table II, the proportion of unbudded cells gradually increases with incubation time and the cells arrest with a heterogeneous size and a large vacuole (vacuole not shown). The proportion of cells that contain a SPA2 patch continually decreases with incubation time and by 72 h the frequency of cells with a SPA2 patch was <0.3%. As above, all of these cells stained with anti-tubulin antibodies indicating that they are permeable to antibodies.

Table II. Frequency of Stationary-phase Cells with SPA2 Patches

Time of culture incubation	Budded	Unbudded cells with SPA2 patch	*n*
h	%	%	
0 (log phase)	69	97	364
24	28	24	163
48	6	4	197
72	1.2	0.4	254

To determine whether *cdc*-arrested and stationary phase cells that lacked a distinctive SPA2 staining region still contain the SPA2 protein, immunoblot analysis was carried out (Fig. 6). Protein extracts from the arrested cells were separated in an SDS-containing gel. Gel blots were prepared and

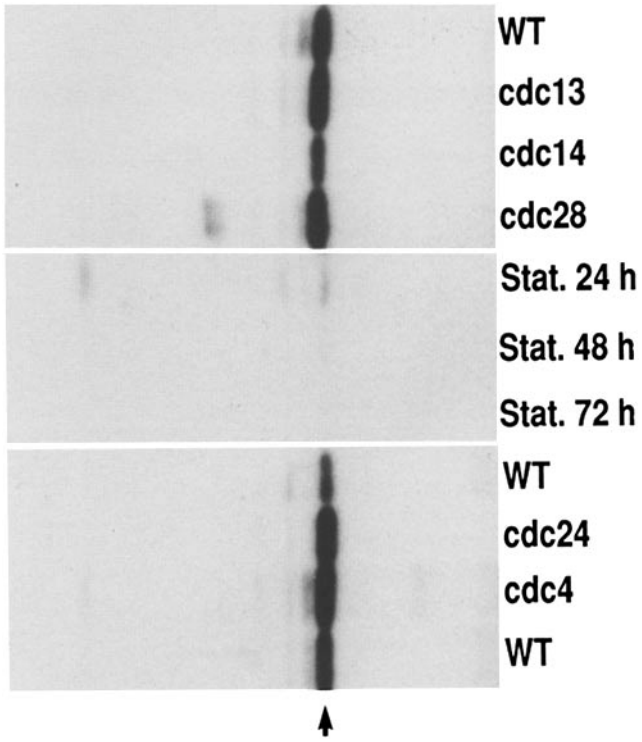

Figure 6. Immunoblot analysis of *cdc*-arrested and stationary phase cells. Protein extracts from arrested cells were prepared, separated in a polyacrylamide gel containing SDS, blotted to nitrocellulose and probed with anti-SPA2 antibodies. The top of the gel corresponds to the right. WT A364A (protein samples at the far ends) is the parent strain background for the various *cdc* mutants except *cdc24*. WT C276 (protein sample next to the *cdc24* sample) is the wild-type parent for that strain. The different mutant strains are described in the legends to Figs. 5 and 7. The arrow indicates the position of the SPA2 protein. The amount of protein loaded from the *cdc14* sample is less relative to the other samples and probably accounts for its reduced signal.

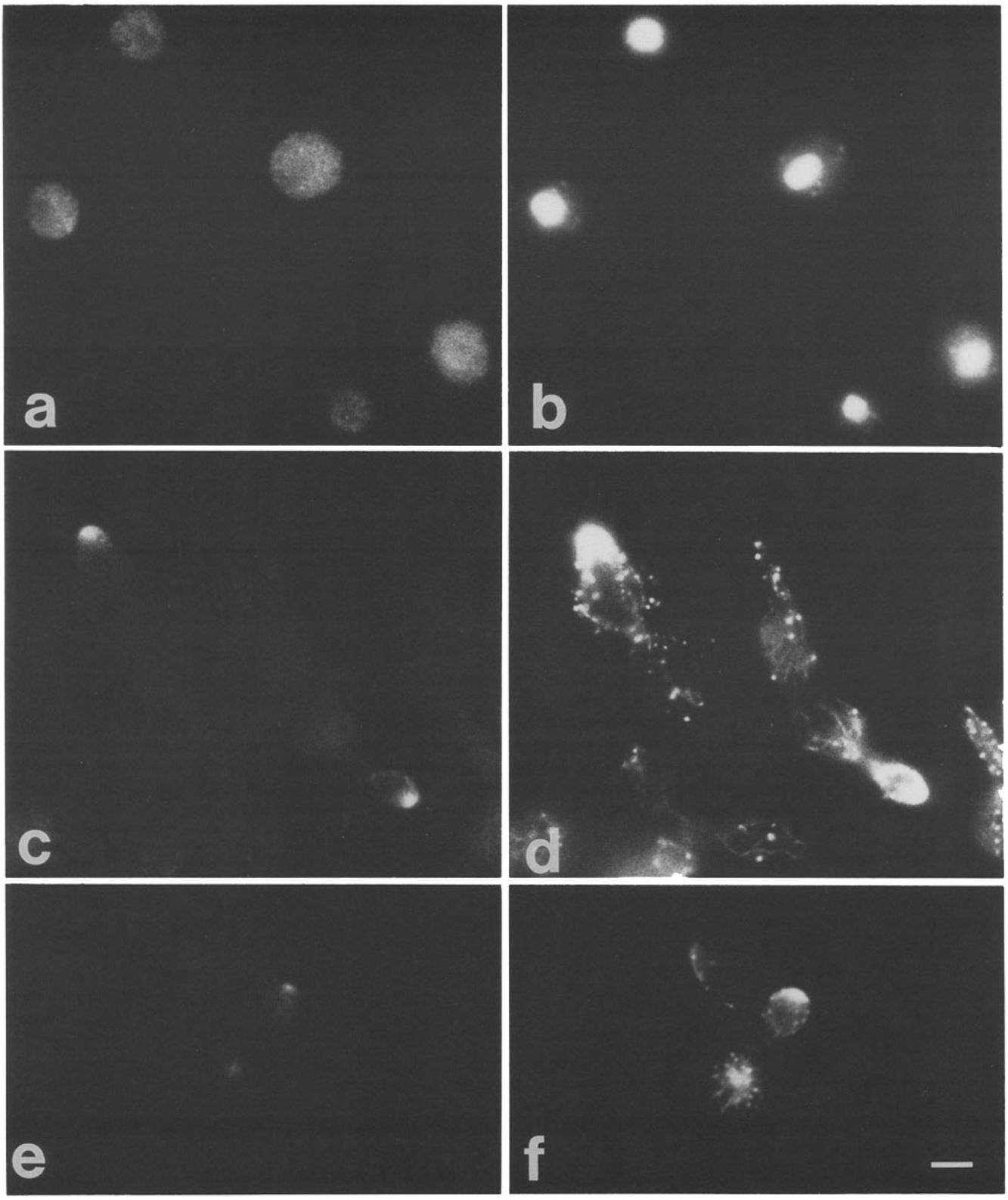

Figure 7. *cdc24-* and *cdc4*-arrested cells stained with anti-SPA2 antibodies. (*a* and *b*) *cdc24-2*-arrested cells (*Y588*). (Similar results were obtained with *cdc24-4* and haploid *cdc24-3* and strains) (*c–f*) *cdc4*-arrested cells (*Y585*). The *cdc4* cells were simultaneously stained with rhodamine-conjugated phalloidin which binds F actin (*d* and *f*). Note the same regions stain with both phalloidin and anti-SPA2 antibodies. Upon lighter exposures the dense actin staining regions are comprised as spots. (*a*, *c*, and *e*) Stain with anti-SPA2 antibodies (*b*) Hoechst 33258 stain of *a*. Bars: (*a* and *b*), ~4 μm; (*c–f*) 2 μm.

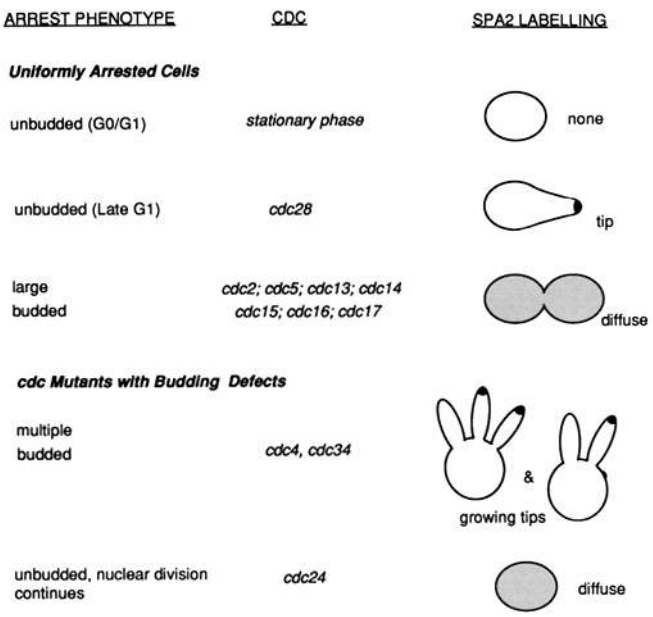

Figure 8. Summary of SPA2 staining in *cdc*-arrested and stationary phase cells.

probed with anti-SPA2 antibodies. As shown for wild-type and *cdc28*-arrested cells, the SPA2 protein migrates as an ~180-kD polypeptide, in agreement with previous results (Snyder, 1989). Cells that arrest as large budded cells, *cdc13* and *cdc14*, still contain copious amounts of the SPA2 protein indicating that the protein is still present but not sharply localized in these cells. Stationary-phase cells gradually lose the SPA2 protein with increased incubation time, indicating that the protein is lost from yeast cells once they exit the cell cycle.

Distribution of the SPA2 Protein in Morphogenic cdc Mutants

To attempt to determine what genes control the distribution of the SPA2 protein, we analyzed *cdc* mutants that affect budding in yeast. *cdc24* mutant cells fail to form buds yet continue to undergo nuclear division forming large multinucleate cells. *cdc24-2*, *cdc24-3*, and *cdc24-4* cells were shifted to the restrictive temperature for 2 h and stained with anti-SPA2 antibodies. As shown in Fig. 7, no SPA2 patches are observed in any of the cells (185 cells examined), although a few very faint regions were observed near the edges of the cell surface in ~5% of the cells. Higher than background staining appears throughout the cell and often at the cell surface. Immunoblot analysis indicates that the SPA2 protein is still present in these cells (Fig. 6) indicating that it is not localized properly. Hence, the CDC24 gene product directly or indirectly controls the localization of the SPA2 protein.

We also examined the distribution of the SPA2 protein in *cdc4-1* and *cdc34-1* cells that form multiple elongated buds at the restrictive temperature. For both mutants, SPA2 antibodies stain the tips of a subset of buds, usually the shorter ones which we expect are in the process of growth (see Fig. 7 for *cdc4* cells). Occasionally a patch on the edge of the cell near one of the buds also stains (Fig. 7 *e*). This patch may correspond to the region where the next bud will form. The regions stained by SPA2 are also stained with rhodamine-conjugated phalloidin and indicate that actin spots are in these regions. A summary of the SPA2 localization pattern in each of the cdc mutants is shown in Fig. 8.

Relationships between Tubulin, the SPA2 Protein, and Actin in the Maintenance of Cell Polarity

Since the SPA2 protein, actin spots, and the ends of microtubules are all present in the same region of yeast cells, we used appropriate mutants to determine the relationships between these different proteins/components (i.e., which proteins control the distribution of the other proteins/components).

spa2-2 and *spa2-3* mutant cells contain a large deletion of the *SPA2* gene. These cells grow at normal rates during vegetative growth, but contain slightly altered budding patterns and are defective in projection formation of yeast cells preparing to mate. When vegetatively growing *spa2-2* and *spa2-3* mutant cells were stained with anti-tubulin antibodies and rhodamine-conjugated phalloidin, the distribution of microtubules and actin appeared similar to wild type. The presence of microtubule bundles that intersect the incipient bud site in unbudded cells could not be scored, because of the absence of the SPA2 staining region in these cells. However, long microtubules usually extended into small budded cells. Actin spots also accumulated near one end of the cell in the unbudded cells (see Fig. 9 for wild-type staining pattern). Hence, the SPA2 protein does not determine the extension of microtubule ends into small buds, and it does not control the distribution of actin.

Cold-sensitive β-tubulin mutants (*tub2-401*, *tub2-402*, *tub2-403*, *tub2-404*, *tub2-405*, and *tub2-104*) were also shifted to the restrictive temperature (11°C) for various periods of time (Huffaker et al., 1988). The presence and distribution of the SPA2 protein was followed until the cell cycle block at mitosis. More than 50% of the *tub2-401* cells had no visible microtubules within 8 h. Unbudded and budded cells that had lost their microtubules had a SPA2 staining pattern similar to that of wild-type cells indicating that microtubules are not important for the maintenance of SPA2 polarity (data not shown).

The distribution of the SPA2 protein was examined in two actin mutants, *act1-1* and *act1-2* (Novick and Botstein, 1985). At the permissive temperature of 20–22°C many *act1-1* and most *act1-2* cells no longer contain an asymmetric distribution of actin spots; spots are often found in both the mother and the bud. The cells also tend to be very heterogeneous in size with many very large cells present in the population. In general, however, the localization of the SPA2 protein with anti-SPA2 antibodies is similar to that of wild-type even in cells that no longer contain a polarized distribution of actin (Fig. 9, *C* and *D*). After 1 h at the restrictive temperature of 37°C, the actin spots no longer appear polarized in any of the *act1* mutant cells; both mother and daughter cells contain the actin spots. Approximately 60–80% of the *act1-2* cells stained normally with anti-SPA2 antibodies; budded cells contained the SPA2 protein at the tip of the bud, and 25–50% of unbudded cells contain a SPA2 patch. For *act1-1* cells the results were more variable; usually ~20% of the cells had a SPA2 staining patch either at the tip of the bud or on the edge of the cell. However, the fraction of SPA2 staining cells varied from 4 to ~40% depending upon the experiment. We expect that some of this variability was due

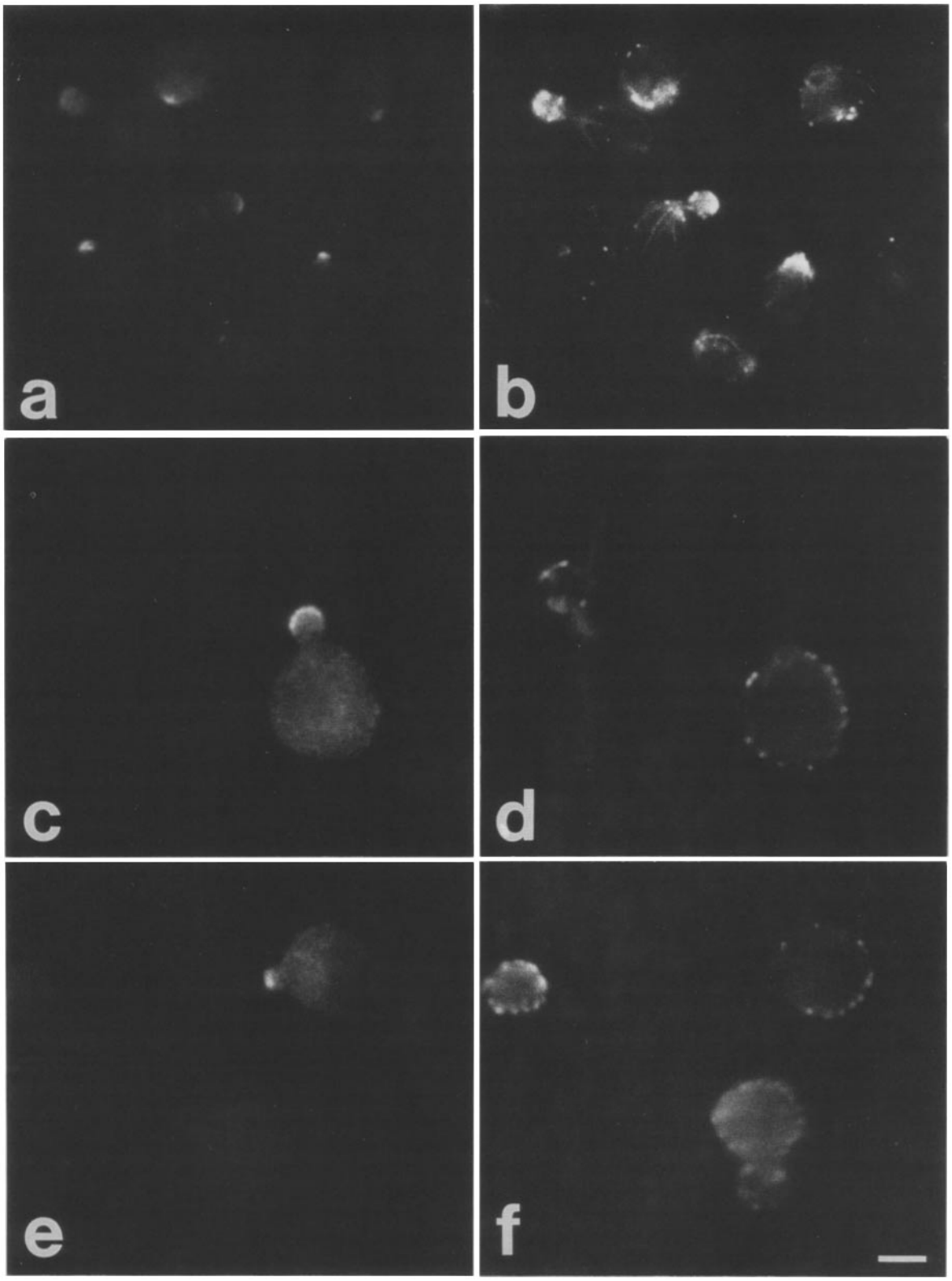

Figure 9. actl and wild-type cells stained with anti-SPA2 antibodies. (*a* and *b*) Wild-type cells (Y603). (*c* and *d*) *actl-2* cells grown at the permissive temperature (*c* and *d*) or those shifted to the restrictive temperature for 1 h (*e* and *f*) were simultaneously stained with anti-SPA2 antibodies and rhodamine-conjugated phalloidin. (*Left*) (*a*, *c*, and *e*) anti-SPA2 antibodies. (*Right*) (*b*, *d*, and *f*) rhodamine-conjugated phalloidin. Bar, ~2.5 μm.

to the loss of cell viability at these restrictive temperatures (Novick and Botstein, 1985). In summary, we conclude that because the SPA2 protein can still localize to its correct location in many of the *act1* mutant cells, that actin is not essential for maintaining the localization of the SPA2 protein. However, actin may still be involved in establishing the polarity of the SPA2 protein. In summary, neither actin nor the SPA2 protein is essential for maintaining of the localization of the other protein, although either protein may still augment the localization of the other.

Discussion

Localization of SPA2 throughout the Yeast Cell Cycle

The data presented above demonstrate that the SPA2 protein localizes to sites involved in polarized growth in yeast: in a patch on the end of unbudded cells, expected to be the incipient bud site, and at the bud tip in budded cells, where cell growth occurs (Adams and Pringle, 1984). Some cells with a very large bud no longer stain at the bud tip, but rather have diffuse staining throughout the entire bud; indeed cdc mutants that arrest at the large budded stage (*cdc13* and *cdc14*) have this pattern and still contain the SPA2 protein. Hence, in many cases when the bud reaches maximal size the SPA2 protein becomes delocalized within the bud. For many large budded cells at cytokinesis, staining is still observed at the tip of the bud as well as the bud neck (not shown). Thus, either these buds have not reached maximal size or the SPA2 protein does not always become delocalized from the bud tip before cytokinesis.

In the A364A strain background used in these studies, staining is readily observed at the bud neck at cytokinesis. This was not observed in our previous experiments probably for a combination of two reasons. First, additional experiments with S288C strains reveals that they also stain at the bud neck at cytokinesis, albeit at a much lower frequency (<1% of large budded), and with a much reduced intensity. Second, immunofluorescence conditions have now been optimized for staining yeast cells with anti-SPA2 antibodies that allow easy detection of the SPA2 protein. Staining at the bud neck is probably not due to reaction of the affinity-purified antibodies with residual cell wall components (Haarer and Pringle, 1987) for four reasons. First, the staining at the neck is relatively uniform in size from one staining cell to the next and from one experiment to the next. Second, the staining appears to lie within the cell as opposed to outside the cell. Third, only budded cells with fully separated nuclei stain at the neck; this is a small fraction of the total budded cells (~2%). Finally, no staining is observed in the *spa2-2* or *spa2-3* mutant cells. Thus, the staining at the site of cytokinesis is due to the presence of the SPA2 protein.

Further evidence that the SPA2 protein plays a role in cytokinesis comes from analysis of *spa2* mutant cells. During microdissection experiments (Snyder, 1989), many *spa2* cells with new buds have not completely separated from their previous daughter cells. This defect is slight and may primarily affect the cell wall, because microscopic examination of *spa2* spheroplasts does not reveal an increase in large budded cells over wild type strains.

Both actin and the SPA2 protein localize to the site of cytokinesis and sites of cell growth (Adams and Pringle, 1984; Drubin, 1990; Kilmartin and Adams, 1984; Novick and Botstein, 1985). Presumably membrane growth and/or structural changes occur at the neck during cytokinesis; these may have features in common with the morphogenic events that occur at sites of cell growth.

A small fraction of unbudded cells contain two SPA2 patches. In haploid cells these patches reside adjacent to each other while in diploid cells they usually lie at opposite sides of the cell, although occasionally they are adjacent to each other. Usually one patch is brighter than the other and microtubules intersect the brighter patch. A simple explanation for the two patches is that one represents the SPA2 site that remains from cytokinesis while the other represents the new bud site that is about to form. The weaker staining patch probably corresponds to the patch remaining from cytokinesis because this region is much weaker than the SPA2 staining region in late G1 cells or newly budded cells. Diploid cells with two patches comprise ~5–10% of the unbudded cells in the A364A background. In S288C strains such cells are difficult to find (<1% of the unbudded cells), presumably because these cells either do not always stain during cytokinesis or their presence at cytokinesis is more transient.

Establishment of the SPA2 Polarity Patch during G1 and the Temporal Order of Events Involving SPB/Nuclear Orientation, and Microtubule Interaction with the Incipient Bud Site

During G1 in haploid cells several events must occur: (*a*) establishment of the incipient bud site; (*b*) SPB migration or nuclear rotation so that the SPB faces the incipient bud site; and (*c*) interaction of the microtubule bundle with the newly formed buds. Analysis of synchronized cells (Figs. 2 and 3) indicates that cells that do not stain with SPA2 antibodies appear at the beginning of G1. These cells quickly disappear from the population suggesting that the SPA2 patch forms early in G1. Indeed, based on several criteria described in Materials and Methods we can crudely estimate that the SPA2 patch is established within 5 min after cytokinesis. Since the G1 phase of these yeast strains is 35–40 min, the SPA2 patch is present throughout most of G1.

Since a number of cells in early G1 contain two SPA2 patches it appears that not all cells lose their cytokinesis patch before formation of the new one. Thus, these cells always contain a SPA2 patch. It is also plausible that a significant fraction of the population simultaneously lose the cytokinesis patch and form the incipient bud patch. Because of the transient nature of the cells that do not contain a SPA2 patch, and the difficulty in scoring cells with two patches, it is difficult to precisely quantitate the fraction of cells that undergo each of the different possibilities.

Staining of synchronized cells with rhodamine-conjugated phalloidin indicates that actin, like SPA2, also polarizes to the incipient bud site very early in the cell cycle. Kim et al. (1991) recently reported that another protein, the CDC3 protein, which is involved in formation of rings at the bud neck, arrives at the presumptive bud site well in advance of bud formation. Thus, a number of different proteins that are involved in various aspects of budding begin preparing for bud formation substantially ahead of the actual budding process.

Of particular interest is where in the cell cycle the SPA2 patch appears relative to the SPB/nuclear reorientation and microtubule attachment. From the data presented in Figs. 3

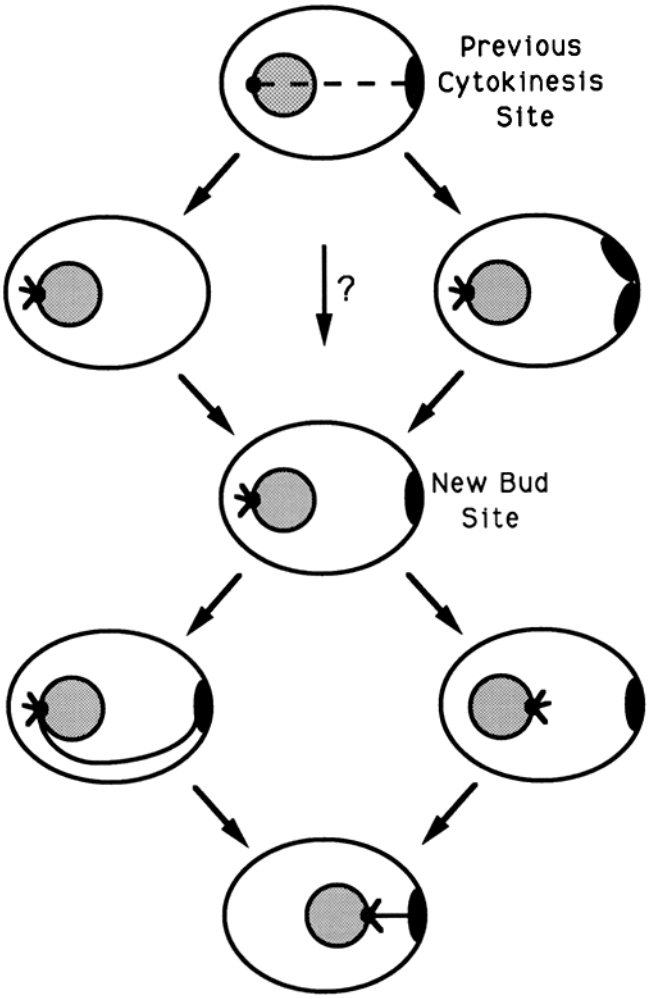

Figure 10. Model for the order of cell cycle events that occur during G1 as described in the text.

C and 4, these events can be organized into a scheme shown in Fig. 10. First, the SPA2 patch is established often while the SPB is still on the distal side of the nucleus (Fig. 4, *B* and *C*); these cells accumulate early in G1. Next, a long extranuclear microtubule bundle intersects the SPA2 staining region (Fig. 4, *D* and *E*); with the exception described below, the accumulation of these cells roughly follows that of the unattached nuclei. Finally, the nucleus rotates (see below) so that the SPB faces the SPA2 staining region, perhaps through its microtubule anchor.

We prefer the hypothesis that the nucleus rotates, as opposed to the SPB migrating through the nuclear envelope, because initially in many of the cells the nucleolus is opposite the SPB (Fig. 4, *B* and *C*). This nucleolus/SPB configuration, which is present in most unbudded cells (Yang et al., 1989; Yang, C. H., and M. Snyder, unpublished), would be preserved if the entire nucleus simply rotated. Alternatively, if the SPB migrated through the nuclear envelope simultaneous migration of the nucleolus would have to occur; a plausible, though potentially more complicated, mechanism.

An additional mechanism that may occur during G1 is that the nucleus may orient towards the SPA2 staining region before attachment. Rapid attachment of a microtubule bundle to the staining region would then lead to attached nuclei. This attachment must be rapid, because except for the earliest timepoint (65 min) very few cells are observed in which the SPB is oriented towards the SPA2 staining region, but do not have a microtubule bundle that intersects the SPA2 staining region. If microtubules are rapidly growing and shrinking from the SPB, then we might expect that when the SPB is oriented towards the SPA2 staining region, attachment will be rapid if a microtubule capture site exists nearby (see below).

The general distribution of cells that have the SPB on the SPA2-distal side of the nucleus and have a microtubule bundle that intersects the SPA2 patch is similar to the distribution of cells that do not have an intersecting microtubule bundle. The broad profile of these distributions may be due to the longer half life of the cells without an intersecting microtubule bundle, relative to the other types of unbudded cells in the population (for example, cells that do not stain with anti-SPA2 antibodies). The number of cells that have an intersecting microtubule bundle at the 65- and 75-min timepoints is probably slightly larger than expected; these higher numbers may be affected, in part, by cells that have just completed cytokinesis and have not yet dissolved their spindle or SPA2 patch. Indeed, many cells in these two populations appear to have a very straight microtubule bundle that appears to pass through the nucleus, instead of around it. Although such cells may slightly complicate our analysis of this particular class of unbudded cells, the combination of the morphological and kinetic data are certainly consistent with the microtubule attachment pathway presented in Fig. 10.

In summary, our data are consistent with the model that the SPA2 patch forms at the cell periphery very early in G1. Subsequently, microtubule intersection and nuclear rotation quickly occur.

The Cytokinesis Tag Model for Selection of Axial Bud Sites

A variety of proteins have now been identified that localize both to the site of cytokinesis and to the incipient bud site. These include the *CDC3*, *CDC10*, and *CDC12* gene products (Kim et al., 1991), actin (Adams and Pringle, 1984; Drubin, 1990; Kilmartin and Adams, 1984; Novick and Botstein, 1985), and the SPA2 protein. Based on these observations and the observations of cells with double patches, a model can be proposed called here the "cytokinesis tag model" to account for axial budding. In this model we propose that components of the old site, i.e., the cytokinesis site, are involved in establishing the new bud site. This can occur in two ways. First, the old site could serve as a template or nucleator that initiates formation of the new site. Alternatively, components at the old site may simply move over to the next available position on the cell surface and initiate synthesis of a new site. Axial budding occurs 100% in haploid mother cells, but only 70% in haploid daughter cells (Snyder, 1989). Cells that deviate from axial budding may have disassembled their cytokinesis site prior to the formation of the new site.

Distal budding, in which budding occurs 180° away from the site of cytokinesis, might result either by complete disassembly of critical components at the cytokinesis site or by the modification of these components. Budding might then initiate opposite the spindle pole body (Byers, 1981), which in the absence of the reorientation described above, would preferentially lie opposite the cytokinesis site.

According to this model, yeast strains should exist with mutations that disrupt axial budding but do not affect distal budding. This is the case for several mutants including *spa2* mutants (Snyder, 1989) and *bud3* and *bud4* mutants (Chant and Herskowitz, 1991).

There are several mutants of yeast that exhibit random budding. These include *cdc24* (Sloat et al., 1981) and the *bud1*, *bud2*, and *bud5* genes (Chant and Herskowitz, 1991; Chant et al., 1991). According to the model, random budding might occur through mislocalization of the critical bud initiation components. Alternatively, delayed assembly of such components might result in the loss of preferred assembly sites at the cortex; assembly might then occur at random sites or opposite the SPB which itself might become randomly positioned.

The cytokinesis tag model is potentially applicable to other organisms that exhibit polarized divisions (examples: *Caenorhabditis elegans*, Kemphes et al., 1988; plants, Schnepf, 1986).

A Microtubule Capture Site Resides at the Incipient Bud Site

Cells in G1, particularly those in middle and late G1 and *cdc28*-arrested cells, and those just beginning to form a bud, all contain a long extranuclear microtubule bundle that intersects the SPA2 staining region. For many cells in early G1 the microtubule bundle extends all the way around the nucleus and across the cell (Fig. 4, *D* and *E*); such cells are relatively frequent comprising >10% of the unbudded cell population at many of the timepoints. Since the microtubules of many organisms are unstable and undergo periods of rapid growth and shrinkage both in vitro and in vivo (Mitchison and Kirschner, 1984; Schulze and Kirschner, 1988), it is plausible that a microtubule capture site exists in the SPA2 staining region which stabilizes the long bundle in vivo. The SPA2 protein was isolated with anti-spindle pole autoantibodies, and therefore could conceivably interact with the ends of microtubules. However, if the SPA2 protein is such a capture protein, it must not be the only capture site, because *spa2-2* and *spa2-3* mutants still contain microtubule bundles extending to the bud tip of cells with very small buds. Because the SPA2 patch is not present in the *spa2* mutant cells it is not possible to easily determine if the microtubule bundle intersects such a region in unbudded cells. The purpose of a capture site at the nascent bud site might be threefold. First, anchoring of the microtubule end could account for the observed reorientation of the nucleus. Second, microtubules, although not essential for bud formation (Huffaker et al., 1988; Jacobs et al., 1988), may still augment this process. Finally, microtubules that extend in the direction of the bud are presumably important for nuclear migration during G2 (Huffaker et al., 1988; Jacobs et al., 1988).

Genes that Control SPA2 Polarity in Yeast

cdc24 mutants of yeast fail to form buds at the restrictive temperature, and exhibit delocalized chitin over their cell surface and delocalized actin spots near their cell surface (Adams and Pringle, 1984; Sloat et al., 1981). These cells also fail to localize the SPA2 protein indicating that they are defective in positioning a number of proteins important in establishing the bud site. *act1-1* and *act1-2* mutants of yeast also fail to localize chitin at the restrictive temperature. However, many of these mutant cells still localize the SPA2 protein to the edge of the cell, indicating that actin is not essential for maintenance of SPA2 localization. However, it is still possible that actin is required for initially establishing SPA2 protein localization or augments the localization of the SPA2 protein since many unstained cells are observed. *spa2* mutants still exhibit polarized localization of actin. Hence, the SPA2 protein is not required either for the establishment or maintenance of the polarity of actin spots. It seems likely that some other cytoskeletal component is important for controlling the polarized distribution of both actin spots and the SPA2 protein. Further analysis of components important for cell morphogenesis in yeast may reveal the critical components.

We thank Dr. F. Solomon for providing anti-tubulin antibodies, Drs. L. Hartwell, T. Huffaker, P. Novick, and J. Pringle for providing yeast strains, and C. Copeland, C. Costigan, K. Madden, and B. Rockmill for useful comments on the manuscript.

This work was supported by National Institutes of Health (NIH) grant GM36494 and used equipment purchased with Pew Scholar funds. B. D. Page was supported by NIH training grant HD 07180.

Received for publication 12 February 1991 and in revised form 8 April 1991.

Adams, A. E. M., and J. R. Pringle. 1984. Relationship of actin and tubulin distribution to bud growth in wild-type and morphogenetic-mutant Saccharomyces cerevisiae. *J. Cell Biol.* 98:934–945.

Adams, A. E. M., D. I. Johnson, R. M. Longnecker, B. F. Sloat, and J. R. Pringle. 1990. *CDC42* and *CDC43*, two additional genes involved in budding and the establishment of cell polarity in the yeast *Saccharomyces cerevisiae*. *J. Cell Biol.* 111:131–142.

Bond, J. F., J. L. Fridovich-Keil, L. Pillus, R. C. Mulligan and F. Solomon, 1986. A chicken-yeast chimeric β-tubulin protein is incorporated into mouse microtubules in vivo. *Cell.* 44:461–468.

Burnette, W. N. 1981. "Western blotting": electrophoretic transfer of proteins from sodium dodecyl sulfate-polyacrylamide gels to unmodified nitrocellulose and radiographic detection with antibody and radioiodinated protein A. *Anal. Biochem.* 112:195–203.

Byers, B. 1981. Cytology of the yeast life cycle. *In* The Molecular Biology of the Yeast *Saccharomyces*: Life Cycle and Inheritance. Vol. 1. J. N. Strathern, E. Jones, and J. Broach, editors. Cold Spring Harbor Laboratory, Cold Spring Harbor, NY. 97–142.

Chant, J., and I. Herskowitz. 1991. Genetic control of bud site selection in yeast by a set of gene products that comprise a morphogenetic pathway. *Cell.* In press.

Chant, J., K. Corrado, J. R. Pringle, and I. Herskowitz. 1991. The yeast *BUD5* gene, which encodes a putative GDP-GTP exchange factor, is necessary for bud site-selection and interacts with bud formation gene BEM1. *Cell.* In press.

Drubin, D. G. 1990. Actin and actin binding proteins in yeast. *Cell. Motil. Cytoskeleton.* 15:7–11.

Freifelder, D. 1960. Bud position in *Saccharomyces cerevisiae*. *J. Bacteriol. (Lond.).* 124:511–523.

Gehrung, S., and M. Snyder. 1990. The *SPA2* gene of *Saccharomyces cerevisiae* is important for pheromone-induced morphogenesis and efficient mating. *J. Cell Biol.* 111:1451–1464.

Haarer, B., and J. R. Pringle. 1987. Immunofluorescence localization of the *Saccharomyces cerevisiae* CDC12 gene product to the vicinity of the 10 nm filaments in the mother-bud neck. *Mol. Cell. Biol.* 7:3678–3687.

Hartwell, L. H. 1974. *Saccharomyces cerevisiae* cell cycle. *Bacteriol. Rev.* 38:164–198.

Hayashibe, M., and S. Katohda. 1973. Initiation of budding and chitin-ring. *J. Gen. Appl. Microbiol.* 19:23–39.

Huffaker, T. C., J. H. Thomas, and D. Botstein. 1988. Diverse effects of β-tubulin mutations on microtubules formation and function. *J. Cell Biol.* 106:1997–2010.

Jacobs, C. W., A. E. M. Adams, P. J. Szaniszlo, and J. R. Pringle. 1988. Functions of microtubules in the *Saccharomyces cerevisiae* cell cycle. *J. Cell Biol.* 107:1409–1426.

Kemphues, K. J., J. R. Priess, D. G. Morton, and N. Cheng. 1988. Identification of genes required for cytoplasmic localization in early *C. elegans* embryos. *Cell.* 52:311–320.

Kilmartin, J. V., and A. E. M. Adams. 1984. Structural rearrangements of tubulin and actin during the cell cycle of the yeast Saccharomyces. *J. Cell Biol.* 98:922–933.

Kilmartin, J. V., B. Wright, and C. Milstein. 1982. Rat monoclonal antitubulin antibodies derived by using a new nonsecreting rat cell line. *J. Cell Biol.* 93:576–582.

Kim, H. B., B. K. Haarer, and J. R. Pringle. 1991. Cellular morphogenesis in the *Saccharomyces cerevisiae* cell cycle: localization of the CDC3 gene product and the timing of events at the budding site. *J. Cell Biol.* 112:535–544.

Laemmli, U. K. 1970. Cleavage of structural proteins during the assembly of the head of bacteriophage T4. *Nature (Lond.).* 227:680–685.

Mitchison, T., and M. Kirschner. 1984. Dynamic instability of microtubule growth. *Nature (Lond.).* 312:237–242.

Novick, P., and D. Botstein. 1985. Phenotypic analysis of temperature-sensitive yeast actin mutants. *Cell.* 40:405–416.

Pringle, J. R., and L. H. Hartwell. 1981. The *Saccharomyces cerevisiae* cell cycle. *In* The Molecular Biology of the Yeast *Saccharomyces*: Life Cycle and Inheritance. Vol. 1. J. N. Strathern, E. Jones, and J. Broach, editors. Cold Spring Harbor Laboratory, Cold Spring Harbor, NY. 97–142.

Schnepf, E. 1986. Cellular polarity. *Annu. Rev. Plant Physiol.* 37:23–47.

Schulze, E., and M. Kirschner. 1988. New features of microtubule behaviour observed *in vivo*. *Nature (Lond.).* 334:356–359.

Sherman, F., G. R. Fink, and J. B. Hicks. 1986. Methods in Yeast Genetics. Cold Spring Harbor Laboratory, Cold Spring Harbor, NY. 186 pp.

Sloat, B. F., and J. R. Pringle. 1978. A mutant of yeast defective in cellular morphogenesis. *Science (Wash. DC.).* 200:1171–1173.

Sloat, B. F., A. Adams, and J. R. Pringle. 1981. Roles of the *CDC24* gene product in cellular morphogenesis during the *Saccharomyces cerevisiae* cell cycle. *J. Cell Biol.* 89:395–405.

Snyder, M. 1989. The SPA2 protein of yeast localizes to sites of cell growth. *J. Cell Biol.* 108:1419–1429.

Trueheart, J., J. D. Boeke, and G. R. Fink. 1987. Two genes required for cell fusion during yeast conjugation: evidence for a pheromone induced surface protein. *Mol. Cell. Biol.* 7:2329–2334.

Yang, C. H., E. J. Lambie, J. Hardin, J. Craft, and M. Snyder. 1989. Higher order structure is present in the yeast nucleus: autoantibody probes demonstrate that the nucleolus lies opposite the spindle pole body. *Chromosoma (Berl.).* 98:123–128.